

MEASUREMENT AND INTERPRETATION OF ELECTRON ANGLE AT MABE BEAM STOP

T. W. L. Sanford, P. D. Coleman, and J. W. Poukey  
Sandia National Laboratories  
Albuquerque, NM 87185

Abstract

This analysis shows that radiation measurements combined with a sophisticated simulation provides a simple but powerful tool for estimating beam temperature in intense pulsed annular electron-beam accelerators. Specifically, the mean angle of incidence of a 60 kA, 7 MeV annular electron-beam at the beam stop of the MABE accelerator and the transverse beam temperature are determined. The angle is extracted by comparing dose profiles measured downstream of the stop with that expected from a simulation of the electron/photon transport in the stop. By calculating and removing the effect on the trajectories due to the change in electric field near the stop, the beam temperature is determined. Such measurements help give insight to beam generation and propagation within the accelerator.

Introduction

MABE (Megamp Accelerator and Beam Experiment), shown schematically in Fig. 1, is a multistage linear electron accelerator. MABE uses a foilless diode immersed in a 20 kG magnetic field to generate a pulsed 60 kA annular electron-beam that is then accelerated to energies of 7 MeV.<sup>1,2</sup> At the end of the last acceleration stage, the electron beam is stopped by a graphite or Ta/graphite target, producing a radiation pulse of width 17 ns (FWHM). The radiation pattern downstream of this target is a sensitive function of the incident electron angle. Understanding the origin of this angle and how to control it is needed in order to design a target configuration that will produce the desired radiation pattern.

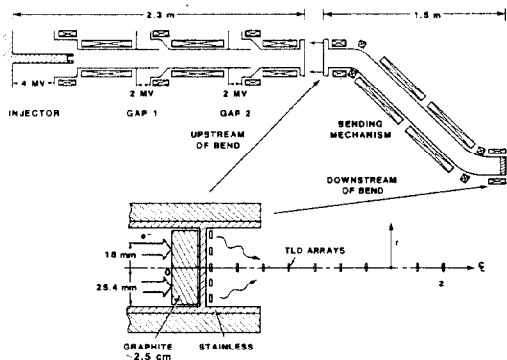


FIGURE 1. MABE and Target Geometry.

In support of this goal, we have made extensive TLD (thermal luminescent detector) measurements of the dose downstream of the target. In this paper, these measurements are compared to those expected for different electron trajectories and KE (kinetic energies) at the target, using the Monte Carlo electron-photon transport code CYLTRAN.<sup>3</sup> From this comparison, the mean polar-angle of the incident electrons is extracted. Non-normal incidence is expected, because as the beam impinges on the target, its radial electric-field,  $E_r$ , is shorted (Fig. 2), causing the beam to self-pinch radially inward. As it pinches, the beam experiences an azimuthal rotation, due to the  $\vec{V}_r \times \vec{B}_z$  force, generated by the strong axial-field,  $B_z$ . Thus, the angle of the electrons incident on the target, and hence the radiation pattern downstream of the target, are altered. In this paper, the magnitude of this P/R (pinch/rotation) effect is also evaluated using both

(Adler Miller) model.<sup>5</sup> Comparison of the mean polar-angle inferred from the radiation measurements with that expected for the P/R effect enables us to set a limit on the mean transverse-velocity of the beam at the target. Such motion imparts cyclotron rotation on the beam electrons, which also alters their angle. This type of motion may be introduced at the diode injector or in the downstream accelerating gaps.

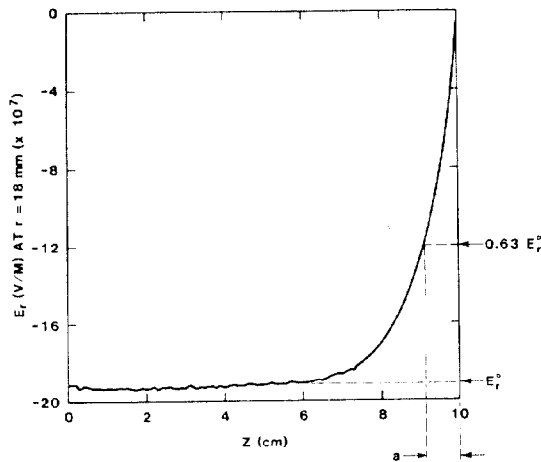


FIGURE 2. Radial Electric Field Near MABE Target Located At 10cm.

The paper is divided into four sections. In the first, the beam and target parameters are defined; in the second, the measurement of the incident angle is discussed; in the third, the P/R effect is evaluated; and in the fourth, a limit on the mean transverse-velocity of the beam is estimated.

I. Beam and Beam Stop

The radiation measurements were made parasitically with the development of the accelerator. Under these conditions, the annular beam had a peak current of 60 kA and was accelerated typically to a peak KE of 7 MeV. The average current and KE were  $45 \pm 15$  kA and  $4 \pm 0.8$  MeV, respectively. Additionally, measurements were made downstream of an added bending section located at the exit of the accelerator. Under these conditions, the average current dropped to  $23 \pm 8$  kA at the exit of the bending section. The outer radius of the annulus was roughly 2 cm and had a width of 2 mm at the cathode. The axial guiding magnetic-field was nominally 20 kG. However, 10 cm upstream of the target, the field was measured to increase 25% from 20 kG to 25 kG just upstream of the target, falling rapidly to  $23 \pm 3$  kG at the target. The targets used were typically either graphite blocks of 2.5 cm thickness or a Ta plate of thickness 0.15 cm placed just upstream of the graphite. The thickness of graphite was sufficient to range-out the electrons and the Ta was used to optimize the radiation output.<sup>6</sup>

II. Mean Angle of Incidence

Forster and colleagues<sup>7</sup> have pointed out the utility of measuring the radiation field to determine mean electron angles. Our analysis shows that indeed the dose at one position on the Z axis relative to the dose at another on the axis is sensitive to the angle of incidence at the target. Variation in

incident KE over the range 3 to 8 MeV, on the other hand, produces little variation in this dose ratio.<sup>8</sup> As shall be shown, the P/R effect also shows little sensitivity to KE over this KE range. Accordingly, a measurement of the relative dose-profile along the Z axis can be used to determine the mean electron-angle just upstream of the target, independent of knowing the exact KE. For a given angle, on the other hand, the absolute scale of the dose profile is sensitive to the KE of the beam. The on-axis dose scales roughly as the KE raised to the 2.7 power.<sup>7</sup> Knowing the relative KE spectrum from the V and I waveforms, for example, the absolute KE scale can be checked. This technique confirmed that the peak KE as measured by the voltage monitor agreed with that estimated by the radiation measurements to about 20%.

For the simulation, the electrons were assumed to be uniformly distributed over an annulus with the parameters just quoted (Fig. 3). The electrons were assumed to have a KE obtained from the measured V and I waveforms. In the simulation, two types of electron-angle models were explored and compared with the radiation data: (1) a P/R model where the azimuthal angle,  $\phi$ , equals  $135^\circ$ , and (2) a uniform  $\phi$  model where  $\phi$  is randomly distributed between 0 and  $2\pi$ . The P/R model was motivated by the AM model, which predicts that  $\theta_r$  (the pinch angle) is approximately equal to  $\theta_\phi$  (the rotation angle) for

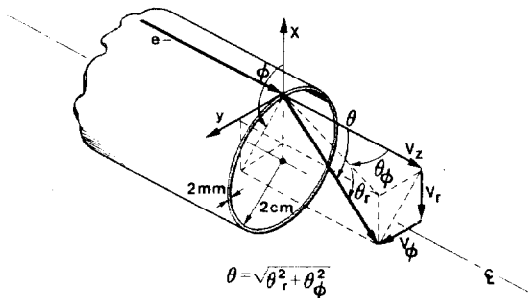


FIGURE 3. Electron Simulation At Target.

our beam parameters. The uniform  $\phi$  model was motivated by noting that the random  $\phi$  trajectory is identical to that arising from cyclotron motion induced by a transverse kick in a distributed KE beam. For both models and all of the measurements taken, the radiation pattern is best described by a  $\theta$  of about  $15^\circ \pm 2^\circ$ . See, for example, Fig. 4.

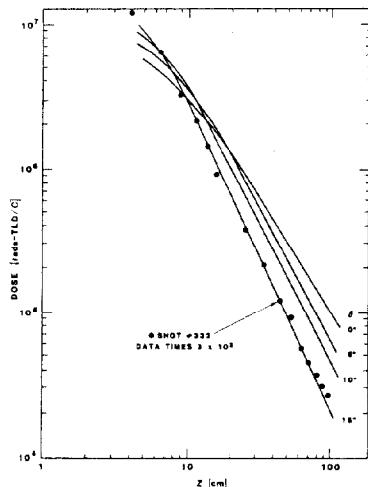


Figure 4. Comparison of Measured Axial Dose Profile with that Simulated as a Function of the Polar Angle in the P/R Model.

At  $15^\circ$ , the P/R and uniform  $\phi$  models give identical Z profiles.

### III. P/R Effect

Before a limit on the mean transverse velocity of the beam can be set, the effect of the P/R needs to be unfolded from the angle measurement. The effect on the polar angle was calculated to be  $6.8^\circ \pm 2^\circ$  using a MAGIC simulation of our beam conditions at  $45 \pm 15$  kA, and  $4.1^\circ \pm 1.4^\circ$  at  $23 \pm 8$  kA. The error arises from our uncertainty in knowing the current and magnetic field at the target. The uncertainty was evaluated by exploring the sensitivity of the calculation to beam parameters that bracketed the measured ones. The results of the simulation are shown in Table 1 and Fig. 5 for the 60 kA simulation at 5.4 MeV.

Table 1. Theoretical Target Parameters as a Function of Different Incident Beam Parameters.

| Beam Parameters |          |                     | Target Parameters |                  |                     |                      |
|-----------------|----------|---------------------|-------------------|------------------|---------------------|----------------------|
| I (kA)          | KE (MeV) | B <sub>z</sub> (kG) | $\Delta r$ (mm)   | $\theta_r$ (deg) | $\theta_\phi$ (deg) | $\theta^{P/R}$ (deg) |
| 70              | 5.4      | 20                  | 1.3               | 5.0              | 5.5                 | 7.4                  |
| 30              | 5.4      | 20                  | 0.46              | 2.4              | 3.4                 | 4.2                  |
| 60              | 3.4      | 20 + 25*            | 3.3               | 4.1              | 8.2                 | 9.2                  |
| 60              | 5.4      | 20 + 25             | 4.0               | 4.3              | 8.6                 | 9.6                  |
| 60              | 9.4      | 20 + 25             | 3.8               | 8.2              | 5.5                 | 9.9                  |
| 60**            | 5.4      | 20 + 25             | 4.4               | -12.7            | 14.0                | 18.9                 |

\*B<sub>z</sub> field described in text.

\*\*Electrons given  $10^\circ$  transverse kick at injection.

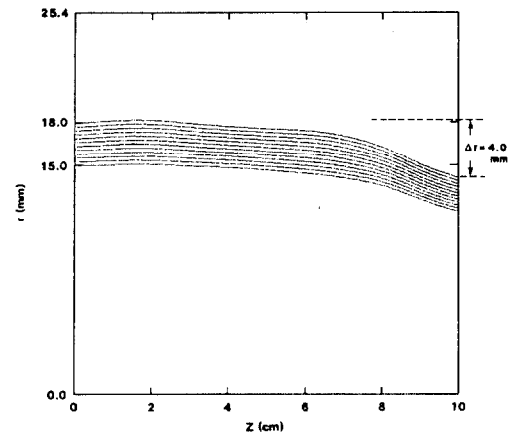


Figure 5. Radial Beam Profile Near the Target for an Incident 60 kA Beam in the Nonuniform Guiding Field Described in the Text. The Target is Located at 10 cm and the KE of the Beam is 5.4 MeV.

Basically, the effect scales roughly with I, is insensitive to KE over the range 3 to 9 MeV, and  $\theta_r$  has roughly the same magnitude as  $\theta_\phi$  for uniform B<sub>z</sub> fields. These results can be intuitively understood by using the AM model to estimate the contraction in the outer radius of the beam at the target (Fig. 5) due to shorting E<sub>r</sub>

$$\Delta r = \frac{2Ia^2}{I_r c} \frac{1}{\left[1 + \frac{a^2 \Omega^2}{\gamma^2 c^2}\right]}, \quad (1)$$

the following linear approximation to estimate  $\theta_r$

$$\theta_r \sim \frac{\Delta r}{a}, \quad (2)$$

and the conservation of canonical angular-momentum relation to estimate  $\theta_\phi$

$$\theta_{\phi} - \frac{v_{\phi}}{c} = \frac{1}{2} \frac{\Omega_c r_c^2}{\gamma(r_c - \Delta r)c} \left[ 1 - \frac{\Omega(r_c - \Delta r)^2}{\gamma \Omega_c r_c^2} \right]. \quad (3)$$

In the equations the subscript c refers to the values at the cathode, c is the speed of light,  $\gamma$  is the relativistic factor,  $I_A$  is the Alfvén current,  $\Omega$  is the cyclotron angular frequency, and "a" characterizes the distance over which  $E_r$  decreases to zero at the target (Fig. 2). Equations (1) and (3) give results that agree with the MAGIC calculations to typically better than 20% and give confidence in the numerical analysis.

#### IV. Mean Transverse Velocity

The MAGIC calculation shows that the P/R effect accounts only for a small fraction of the 15° angle measured. The difference can be explained by the mean transverse-velocity that the beam acquires in the diode and accelerating gaps.<sup>9</sup> Such a velocity imparts cyclotron motion to the beam electrons. For example, using MAGIC, Fig. 6 shows the effect on the beam if all the electrons are given an initial kick,  $\theta_T$ , of 10° transverse to the beam axis. From this simulation, the electrons are observed to spiral around the trajectory they would have had without the kick.

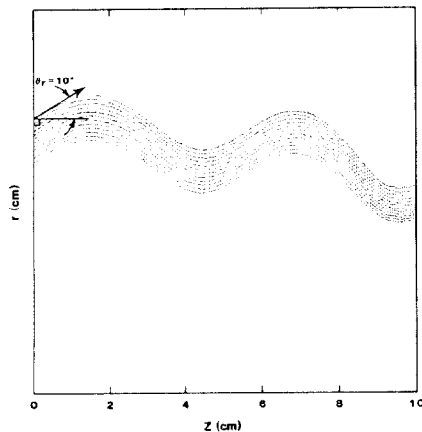


Figure 6. Radial Beam Profile Near the Target Corresponding to the Same Conditions as for Figure 5, Except that the Incident Beam is Injected at 10° with Respect to the Beam Axis.

Generalizing, the total perpendicular velocity that the electrons acquire at the target plane is thus a combination of that received from the P/R effect plus the transverse kick received from the cyclotron oscillations due to the diode and gaps. The phase at the target of the cyclotron oscillation depends on the distance between the cathode and target, the  $B_z$  field, and the KE of the beam electrons. Because the electrons of the actual beam are not monoenergetic, but have a spread of energies, and because the distance from the cathode to target is long relative to the cyclotron wavelength, the phases of the beam electrons become mixed. The average magnitude of the total perpendicular velocity or equivalently the magnitude of the overall polar angle  $\theta$  is thus simply obtained by taking the P/R angle in quadrature with a mean transverse-kick angle,  $\theta_T$ ,<sup>8</sup>

$$\theta^2 = (\theta^{P/R})^2 + \theta_T^2. \quad (4)$$

Using this equation, the measured value of  $\theta$ , and that expected from the P/R effect, the data thus suggests that the beam has received a mean transverse kick of about  $14^\circ \pm 3^\circ$  upstream of the target. This angle, which dominates the P/R effect for either beam condition, corresponds to a mean transverse velocity of 0.23 c. Such inferred transverse motion is indeed characteristic of that possibly given the beam at injection or in subsequent accelerating gaps, as shown by separate MAGIC simulations.<sup>8,9</sup>

#### Summary

A measure of the relative dose along the Z-axis is used to determine the mean electron-angle of an intense annular-beam incident on a target. The measurement is basically independent of the exact beam KE over the range 3 to 8 MeV. The absolute dose, on the other hand, is sensitive to the total beam-energy and angle. Its measure can be used to check the KE scale if the relative spectrum and angle are known. A by-product of the analysis shows that the AM model describes the P/R process to 20% or better when compared to the MAGIC simulation. Lastly, this analysis shows that radiation measurements combined with a sophisticated CYLTRAN simulation provides a simple but powerful tool for estimating electron angles and corresponding beam temperature. Such measurements help give insight to beam generation and propagation within the accelerator.

#### Acknowledgments

We would like to thank W. Beezhold, T. P. Wright, J. A. Halbleib, R. B. Miller, J. J. Ramirez and D. E. Hasti for useful discussions and for their encouragement of this research. R. E. Craven, N. Counts, and A. W. Sharpe are also thanked for their technical support.

#### References

- [1] K. R. Prestwich, D. Hasti, R. B. Miller, and A. W. Sharpe, IEEE Trans. Nucl. Sci. W-30, No. 4 (August 1983) 3155.
- [2] P. D. Coleman, J. J. Ramirez, D. E. Hasti, R. B. Miller, T. W. L. Sanford, J. W. Poukey, A. W. Sharpe, and C. W. Huddle, Bull. Am. Phys. Soc. 29 (October 1984) Paper 4U10, and P. D. Coleman, et al., Paper Y3 this conference.
- [3] J. A. Halbleib and W. H. Vandevender, Sandia National Laboratories SAND74-0030 (December 1982) Albuquerque, New Mexico.
- [4] B. Goplen, R. E. Clark, J. McDonald, W. M. Bollen, User's Manual for MAGIC, Mission Research Corporation, Alexandria, VA (September 1983).
- [5] R. J. Adler and R. B. Miller, J. Appl. Phys 53 (September 1982) 6015.
- [6] T. W. L. Sanford and J. A. Halbleib, IEEE Trans. Nucl. Sci. NS-31, No. 6 (December 1984) 1095.
- [7] D. W. Forster, M. Goodman, G. Herbert, J. C. Martin, and T. Storr, Atomic Weapons Research Establishment, England, SSWA/JCM/714/162 (April 1971).
- [8] T. W. L. Sanford, P. D. Coleman, and J. W. Poukey, Sandia National Laboratories Report SAND1423 (February 1985), Albuquerque, New Mexico.
- [9] J. W. Poukey, P. D. Coleman, and T. W. L. Sanford, Paper U45, this conference; Bull. Am. Phys. Soc. 30 (1985) 987; and Sandia National Laboratories Report SAND84-2652 (March 1985).